ROYAL SOCIETY OF CHEMISTRY

PAPER

Check for updates

On zinc(II) coordination chemistry with furosemide: a journey from a mononuclear complex to a coordination polymer†

Nina Podjed, [ID]ᵃ Zarja Uranjek,ᵃ Romana Cerc Korošec,ᵃ Martina Hrast Rambaher, [ID]ᵇ Majda Golob [ID]ᶜ and Barbara Modec [ID]*ᵃ

In continuation of our studies on zinc(II) coordination chemistry, reactions between the zinc(II) starting material and furosemide were investigated. Furosemide, a well-known pharmaceutical, contains functional groups which could serve as donors in coordination with metal ions. Reactions between zinc oxide or chloride and furosemide in aqueous ammonia solution yielded a mononuclear complex, $[Zn(NH_3)_2(fur)_2]$ (**1**), where fur⁻ stands for deprotonated furosemide. Unfortunately, some reactions produced mixtures of the desired metal complex **1** and by-product, ammonium salt NH_4fur (**2**). To further explore the coordination chemistry of furosemide, quinaldinate (an anion of quinoline-2-carboxylic acid, abbreviated as quin⁻) was introduced into the reaction system, resulting in the formation of a coordination polymer, $[Zn_3(quin)_4(fur)_2]_n \cdot 2nCH_3OH$ (**3**). **1** and **3** were evaluated for their antibacterial properties against Gram-positive and Gram-negative bacteria. Notably, compound **3** exhibited moderate antibacterial activity against *Staphylococcus epidermidis*, representing a promising starting point for the preparation of potential antibacterial zinc(II) complexes.
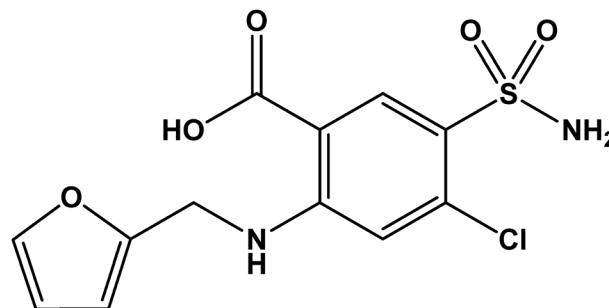
Introduction

Furosemide (IUPAC name: 4-chloro-2-(furan-2-ylmethylamino)-5-sulfamoylbenzoic acid) is a crystalline solid that belongs to a class of sulphonamide derivatives. The molecule contains a chlorine-substituted phenyl ring, a furan ring, a sulphonamide group, an amine group and a carboxyl group (Scheme 1). The latter makes furosemide a weak organic acid, with a pK_a value of 3.8.[1] Furosemide is a potent diuretic used orally in the treatment of edema, caused by cardiac, renal, and hepatic diseases, and in the treatment of hypertension. Furosemide has, like all medicines, some adverse effects. The most common ones of a prolonged use are electrolyte imbalances and dehydration.[2] Furosemide is practically insoluble in water as the solubility at room temperature is less than 0.1 mg mL⁻¹. Its aqueous solubility increases as a function of the pH of the medium.[1] Poor solubility is the consequence of strong intramolecular and intermolecular hydrogen bonding interactions.[3] According to the biopharmaceutics classification system (BCS), furosemide is therefore classified as a class IV drug, which means that it suffers from both low solubility and low permeability.[4] To increase the solubility and hence the bioavailability of furosemide, several tactics have been reported in the literature. Solubility can be improved by solid form selection, for example polymorphs, hydrates, amorphous materials, solvates, salts, cocrystals, solid dispersions, encapsulation in cyclodextrins, nanoparticles, *etc.*[5] A common strategy for improving the solubility is the salt formation as more than 50% of the drugs are marketed as salts.[6] The formation of furosemide salts is possible because of

ᵃ *Faculty of Chemistry and Chemical Technology, University of Ljubljana, Večna pot 113, 1000, Ljubljana, Slovenia. E-mail: barbara.modec@fkkt.uni-lj.si*

ᵇ *Faculty of Pharmacy, University of Ljubljana, Aškerčeva cesta 7, 1000, Ljubljana, Slovenia*

ᶜ *Institute of Microbiology and Parasitology, Veterinary Faculty, University of Ljubljana, Gerbičeva 60, 1000, Ljubljana, Slovenia*

Scheme 1 Structural formula of furosemide.

the carboxyl group. The rational design of cocrystals containing active pharmaceutical ingredients can be used to fine tune and improve the physicochemical properties, mainly poor solubility and stability, without altering their therapeutic effect.[7] The ability of amine, carboxyl, and sulphonamide functional groups to participate in hydrogen bonding allows furosemide to form cocrystals.[8] Based on the information above, it is not surprising that Cambridge Structural Database reports on many crystal structures of furosemide salts and cocrystals.[9]

It is reported that furosemide itself crystallizes in three different polymorphic modifications, labelled as forms I, II and III.[3] In CSD, however, there are as many as ten reports of furosemide crystal structures.[9] A close survey reveals that several are actually of the same polymorph, form I.[10] The structural formula of furosemide (Scheme 1, abbreviated as furH) tells us that conformational polymorphism[11] is to be expected. The molecule contains a rigid anthranilic acid moiety because of the intramolecular N–H⋯O hydrogen bond. The sulphonamide group and the furan ring, on the other hand, are flexible parts and their rotational freedom can lead to different conformers. Form I was determined first.[12] It is the most thermodynamically stable form because of efficient crystal packing and therefore higher density. All forms feature the same hydrogen bonding motif concerning the carboxyl group. In each polymorph, the sulphonamide group exhibits a different hydrogen bonding motif. The conformations are also different, and the biggest difference can be observed in the orientation of the furyl ring. For these reasons, forms I, II, and III can be called conformational and synthon polymorphs of furosemide.[3] A fourth, high-temperature phase is also thought to exist, but its crystal structure remains unknown.[13]

The furosemide functional groups allow coordination with metal ions. To our surprise, there are only two known crystal structures of coordination compounds with deprotonated furosemide reported in CSD.[9] The first one is a four-coordinated copper(II) complex with two deprotonated furosemides bound in a monodentate manner *via* carboxylate oxygens and two methanol molecules.[14] The second one is a six-coordinated zinc(II) complex, $[Zn(fur)_2(H_2O)(2,2'-bipy)]$. In the latter, the deprotonated furosemide is coordinated in two ways: in a monodentate manner and in a bidentate chelating manner *via* both carboxylate oxygens.[15] To fill the gap, our studies on zinc(II) coordination chemistry[16–20] were extended to furosemide. We succeeded in the preparation of two zinc(II) coordination compounds with deprotonated furosemide. Throughout this paper we refer by (free) furosemide or furH to the species with the COOH group, whereas the anionic form, found also in our compounds, is fur⁻ or a furosemide anion and has a COO⁻ functional group. The first compound is a mononuclear complex with the composition $[Zn(NH_3)_2(fur)_2]$ (1). When quinaldinate, an anion of quinoline-2-carboxylic acid, abbreviated as quin⁻, was introduced into the reaction systems, a one-dimensional (1D) coordination polymer with the composition $[Zn_3(quin)_4(fur)_2]_n \cdot 2nCH_3OH$ (3) was obtained. Both compounds were fully characterized using infrared (IR) and nuclear magnetic resonance (NMR) spectroscopies, elemental analyses and single crystal X-ray diffraction analysis. They were also tested for their antibacterial properties against Gram-positive and Gram-negative
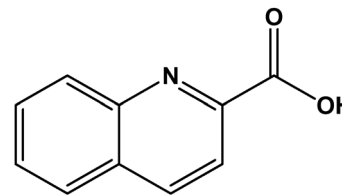
Scheme 2 Structural formula of quinoline-2-carboxylic acid, quinH.

bacteria: *Escherichia coli*, *Staphylococcus aureus*, *Pseudomonas aeruginosa*, *Proteus mirabilis*, *Bacillus subtilis* and *Staphylococcus epidermidis*. Previously, similar zinc(II) complexes were tested on the same bacterial strains.[15]

Experimental

General

All reagents were obtained from commercial sources. Acetonitrile was dried over molecular sieves before use.[21] The starting material $[Zn(quin)_2(H_2O)]$ was synthesized according to a previously reported method.[16] IR spectra were recorded using a Bruker Alpha II FT-IR spectrophotometer with an attenuated total reflection (ATR) module in the 4000–400 cm⁻¹ range. The spectra were presented as obtained, without any corrections. The intensity of the bands was indicated as follows: w = weak, m = medium, s = strong, vs = very strong and vvs = very strong. ¹H NMR spectra were recorded with a Bruker Avance NEO 600 MHz instrument. Deuterated dimethyl sulfoxide $((CD_3)_2SO)$ with 0.03% tetramethylsilane (TMS) standard was used as the solvent. The residual solvent peak of $(CD_3)_2SO$ at 2.50 ppm or the TMS standard at 0.00 ppm was used as a reference for the chemical shifts.[22] The chemical shifts (δ) are given in ppm and the coupling constants (J) in Hz. Multiplicities are denoted as follows: s = singlet, d = doublet, t = triplet, q = quartet and m = multiplet. The spectra were processed using MestReNova software (version 14.2.2).[23] The elemental analyses of carbon, nitrogen, and hydrogen were carried out using a PerkinElmer 2400 II analyser. The TG measurements of 1 were carried out with a Mettler Toledo TGA/DSC1 instrument in a temperature range from 30 to 250 °C. The heating rate was 10 K min⁻¹. During the measurement, the furnace was purged with nitrogen at a flow rate of 50 mL min⁻¹. A 150 μL platinum crucible was used, and the initial mass of the sample was 6.059 mg. The blank curve was subtracted. Evolved gases were transferred to a mass spectrometer (Pfeiffer Vacuum ThermoStar) *via* the 75 cm long heated transfer line. To reduce the water content in the mass spectrometer, the sample was kept at 30 °C for 20 min at the beginning of the measurement. Signals in the range of 2 to 90 *m/z* were collected, of which only the selected ones are shown in Fig. S2 (ESI†). The DSC measurements were performed separately using a Mettler Toledo DSC1 instrument. The sample was carefully weighed using an external Mettler Toledo MX5 microbalance in a 40 μL aluminium pan and covered with a pierced lid. The initial mass of the sample was 1.002 mg. An empty crucible served as a reference. The other instrumental parameters (heating rate, temperature range, purge gas and its flow rate) were the same as for the TG measurement described above.

Preparation of [Zn(NH$_3$)$_2$(fur)$_2$] (1)

Zinc(II) chloride (50 mg, 0.37 mmol), furosemide (243 mg, 0.73 mmol) and an aqueous ammonia solution (15 mL, *ca.* 24%) were added to an Erlenmeyer flask. The mixture was stirred thoroughly until all the solids were consumed (approximately 5 minutes). The flask with the resulting solution was covered with parafilm which was punctured in several places. After a few days of standing under ambient conditions, colourless crystals of [Zn(NH$_3$)$_2$(fur)$_2$] (1) were obtained. The crystals were filtered off. Yield: 178 mg, 64%. IR (ATR, cm^{-1}): 3371w, 3254m, 1612m, 1556m, 1494m, 1449w, 1418w, 1378s, 1358m, 1311m, 1254s, 1191w, 1153s, 1122s, 1070m, 1012m, 966m, 917m, 904w, 885w, 857w, 842w, 811m, 782m, 738s, 689s, 666s, 633s, 622s, 584vs, 558s, 517vvs, 477s, 450m, 424m. ^{1}H NMR ((CD$_3$)$_2$SO with 0.03% v/v TMS, 600 MHz): δ 9.46 (t, J = 5.9 Hz, 1H, NH), 8.50 (s, 1H, CH), 7.59–7.57 (m, 1H, CH), 6.89 (s, 1H, CH), 6.39–6.37 (m, 1H, CH), 6.33 (d, J = 3.2 Hz, 1H, CH), 4.47 (d, J = 5.9 Hz, 2H, CH$_2$) ppm. Elemental analysis calcd for C$_{24}$H$_{26}$Cl$_2$N$_6$O$_{10}$S$_2$Zn (%): C, 37.98; H, 3.45; N, 11.07. Found (%): C, 37.83; H, 3.16; N, 11.03.

Reaction that led to NH$_4$fur (2)

Zinc(II) oxide (50 mg, 0.61 mmol), furosemide (1.19 g, 3.60 mmol) and an aqueous ammonia solution (15 mL, *ca.* 24%) were added to an Erlenmeyer flask. The mixture was stirred thoroughly until all the solids were consumed (approximately 5 minutes). The flask with the resulting solution was covered with parafilm which was punctured in several places. After a few days of standing under ambient conditions, a mixture of crystals of [Zn(NH$_3$)$_2$(fur)$_2$] (1) and NH$_4$fur (2) was obtained. IR for 2 (ATR, cm^{-1}): 3602w, 3346w, 3242m, 2962m, 2835m, 1686w, 1606s, 1555s, 1494m, 1447s, 1414m, 1366s, 1348s, 1302vs, 1257vs, 1191m, 1159vs, 1125s, 1073s, 1013m, 977m, 955s, 915s, 885m, 866m, 826s, 816s, 773m, 743vs, 714s, 684s, 633m, 609s, 599s, 578vvs, 543s, 514vs, 470s, 425s.

Preparation of [Zn$_3$(quin)$_4$(fur)$_2$]$_n$·2nCH$_3$OH (3)

A Teflon container was charged with [Zn(quin)$_2$(H$_2$O)] (100 mg, 0.23 mmol), furosemide (310 mg, 0.94 mmol), acetonitrile (7 mL) and methanol (3 mL). The container was closed and inserted into a steel autoclave, which was heated for 24 h at 105 °C. Afterwards, the reaction mixture was allowed to cool slowly to room temperature. Yellow single crystals of [Zn$_3$(quin)$_4$(fur)$_2$]$_n$·2nCH$_3$OH (3) were filtered off. Yield: 79 mg. Note 1. The solvate was not stable outside the mother liquor and the partial loss of solvent molecules was observed over time. The yield is therefore reported as the mass of solids remaining after approximately 15 minutes of air drying. IR (ATR, cm^{-1}): 3407w, 3276w, 3029w, 1605vs, 1556vs, 1511w, 1497w, 1469s, 1436w, 1415s, 1379s, 1341s, 1298s, 1266s, 1219m, 1165s, 1119m, 1079w, 1055w, 1029s, 1012w, 981w, 968w, 938m, 907m, 877w, 853m, 834w, 805vs, 773vvs, 740s, 728s, 683m, 630m, 615s, 584vvs, 545vs, 519s, 497s, 453s. ^{1}H NMR ((CD$_3$)$_2$SO with 0.03% v/v TMS, 600 MHz): δ 9.10 (t, J = 5.9 Hz, 2H, NH fur$^-$), 8.82–8.74 (m, 6H, quin$^-$), 8.71–8.66 (m, 1H, quin$^-$), 8.60 (s, 1H, quin$^-$), 8.45 (s, 2H, CH fur$^-$), 8.39 (d, J = 8.4 Hz, 3H, quin$^-$), 8.35–8.30 (m, 1H, quin$^-$), 8.20–8.16 (m, 3H, quin$^-$), 8.13–8.09 (m, 1H, quin$^-$), 7.96 (s, 3H, quin$^-$), 7.84–7.76 (m, 4H, quin$^-$), 7.72 (s, 1H, quin$^-$), 7.58 (s, 2H, CH fur$^-$),

7.19 (s, 4H, NH$_2$ fur$^-$), 6.86 (s, 2H, CH fur$^-$), 6.39–6.36 (m, 2H, CH fur$^-$), 6.26 (s, 2H, CH fur$^-$), 4.45 (s, 4H, CH$_2$ fur$^-$), 4.10 (q, J = 5.2 Hz, 2H, CH$_3$OH), 3.17 (d, J = 5.2 Hz, 6H, CH_3OH) ppm. Elemental analysis calcd for C$_{66}$H$_{52}$Cl$_2$N$_8$O$_{20}$S$_2$Zn$_3$ (%): C, 49.29; H, 3.26; N, 6.97. Found (%): C, 48.60; H, 2.74; N, 6.95. Note 2. The elemental analysis data slightly differ from the theoretical values due to the instability of the solvate.

X-ray structure analysis

Single-crystal XRD data were obtained using an Agilent SuperNova diffractometer with a copper X-ray source (Cu-K$_\alpha$, λ = 1.54184 Å) at 150 K. Each crystal was attached to the tip of a glass fibre with silicone grease and then positioned on the goniometer head. CrysAlis PRO[24] was used for data processing. Crystal structures were solved using the methods implemented in ShelXT[25] within Olex^2 software.[26] Crystal structure refinement was performed using the least squares methods in ShelXL.[27] Anisotropic displacement parameters were determined for all non-hydrogen atoms. All hydrogens on heteroatoms were located from residual electron density and isotropically refined. The remaining hydrogen atoms were added in calculated positions. Data analysis was performed using Platon,[28] and images were generated with Mercury.[29] All crystal structures were deposited with the Cambridge Crystallographic Data Centre (CCDC) and assigned the deposition numbers: 2420534 (1), 2420535 (2) and 2420536 (3).† The crystallographic data for 1–3 are summarized in Table 1.

Antibacterial activity

Antimicrobial testing was carried out by the broth microdilution method in a 96-well U plate format following the CLSI guidelines and European Committee for Antimicrobial Susceptibility Testing recommendations. The bacterial suspension of the specific bacterial strain equivalent to the 0.5 McFarland turbidity standard was diluted with a cation-adjusted Mueller Hinton broth with *N*-tris(hydroxymethyl)methyl-2-aminoethanesulfonic acid buffer (Thermo Fisher Scientific) to obtain a final inoculum of 10^5 CFU mL^{-1}. Compounds dissolved in DMSO and inoculum were mixed together and incubated for 20 h at 35 °C. After incubation, the minimal inhibitory concentration (MIC) values were determined by visual inspection as the lowest dilution of compounds showing no turbidity. The MICs were determined against *S. aureus* (ATCC 29213), *E. coli* (ATCC 25922), *P. aeruginosa* RDK 184 (DSM 939; ATCC 15442), *P. mirabilis* (RDK 064, DSM 788), *B. subtilis* (RDK 108, WDCM 00003) and *S. epidermidis* (RDK 065, WDCM 000065) bacterial strains. Tetracycline was used as a positive control on every assay plate.

Results and discussion

Synthetic considerations

In order to prepare zinc(II) coordination compounds with furosemide, simple reaction systems have been designed. Zinc(II) oxide or chloride was combined with furosemide in acetonitrile, methanol or their mixtures. In the case of the room temperature reactions, almost all metal starting materials remained intact. When harsher

Table 1 Crystallographic data for **1–3**

	[Zn(NH$_3$)$_2$(fur)$_2$] (**1**)	NH$_4$fur (**2**)	[Zn$_3$(quin)$_4$(fur)$_2$]$_n$·2nCH$_3$OH (**3**)
Empirical formula	C$_{24}$H$_{26}$Cl$_2$N$_6$O$_{10}$S$_2$Zn	C$_{12}$H$_{14}$ClN$_3$O$_5$S	C$_{66}$H$_{52}$Cl$_2$N$_8$O$_{20}$S$_2$Zn$_3$
Formula weight	758.90	347.77	1608.28
Crystal system	Monoclinic	Monoclinic	Monoclinic
Space group	$C2/c$	$P2_1/c$	$I2/a$
T [K]	150.00(10)	150.00(10)	150.00(10)
λ [Å]	1.54184	1.54184	1.54184
a [Å]	21.5516(5)	8.18826(7)	21.0265(2)
b [Å]	4.83840(10)	4.75496(4)	9.30170(10)
c [Å]	28.6806(7)	36.8598(3)	34.3660(3)
α [°]	90	90	90
β [°]	93.393(2)	91.2793(8)	93.7000(10)
γ [°]	90	90	90
V [Å^3]	2985.43(12)	1434.78(2)	6707.37(11)
Z	4	4	4
D_{calc} [g cm^{-3}]	1.688	1.610	1.593
μ [mm^{-1}]	4.684	3.997	3.263
Collected reflections	9361	46249	25467
Unique reflections	2991	2916	6803
Observed reflections	2564	2863	6471
R_{int}	0.0487	0.1338	0.0311
R_1 ($I > 2\sigma(I)$)	0.0358	0.0407	0.0318
wR_2 (all data)	0.0956	0.1143	0.0836

reaction conditions were applied, *i.e.*, a prolonged heating at 105 °C in autoclaves, an unidentified microcrystalline solid was obtained. Its infrared and ^{1}H NMR spectra suggest this compound to be a zinc(II) complex with a furosemide anion and ammonia. As observed in previous studies, ammonia forms upon the acetonitrile hydrolysis.[20] Despite numerous attempts to obtain well-diffracting crystals of this compound, we have not been successful. Thus, an alternative synthetic approach was undertaken: keeping the reactants' ratio the same, aqueous ammonia was used as a solvent. This reaction medium served another purpose: ammonia acted as a base which effectively deprotonated the furosemide COOH group, producing thereby a form of furosemide which could act as a ligand. Slow evaporation of the resulting solution under ambient conditions gave large colourless crystals of [Zn(NH$_3$)$_2$(fur)$_2$] (**1**), a four-coordinated zinc(II) complex with ammonia and a furosemide anion. Some reactions produced mixtures of the desired metal complex **1** and ammonium salt, NH$_4$fur (**2**). The co-crystallization of the ammonium salt not only contaminated the solid product, but it also diminished the amount of the available furosemide ligand. The thermal stability of **1** was monitored by thermal analysis up to 250 °C (ESI,† Fig. S1 and S2). A major decomposition process starts at approximately 180 °C. The gaseous products were analysed by mass spectrometry, which confirmed the formation of ammonia (m/z = 17 and 16), carbon dioxide (m/z = 44) and sulphur dioxide (m/z = 64 and 48).

In some reactions, [Zn(quin)$_2$(H$_2$O)] (quin$^-$ stands for quinaldinate, the anionic form of quinoline-2-carboxylic acid, shown in Scheme 2) was used as a starting compound.[30] By introducing quinaldinate, we hoped to restrict the chemical space and gain control over the reaction outcome. Namely, quinaldinate is known to preferentially bind in a *N,O*-bidentate chelating manner.[9] The choice of this ligand was governed by our previous success with it.[17,18,20] The [Zn(quin)$_2$(H$_2$O)] reaction with furosemide was carried out in the acetonitrile/methanol mixture at 105 °C in an autoclave.

[Zn$_3$(quin)$_4$(fur)$_2$]$_n$·2nCH$_3$OH (**3**), a one-dimensional coordination polymer, was obtained when the molar ratio of zinc(II) to furosemide was 1:4 and only a certain solvent mixture was used (see the Experimental section for details). The reaction is given by the equation:

$$3[Zn(quin)_2(H_2O)] + 2furH + 2CH_3OH$$
$$\rightarrow [Zn_3(quin)_4(fur)_2]\cdot 2CH_3OH + 2quinH + 3H_2O$$
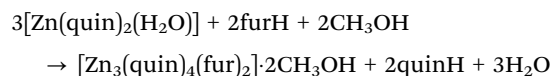
The isolation of **3** proved highly sensitive also to the reactants' ratio. For example, by using a stoichiometric zinc(II)-to-furosemide ratio, **3** was not isolated. Instead, almost all metal starting materials remained unconsumed. In this reaction, the most likely base which deprotonated furosemide was quinaldinate, bound in a *N,O*-bidentate chelating manner to zinc(II). The fact that one third of quinaldinates chose the proton over the metal ion shows its reluctance to act in this way. Apparently both, severe reaction conditions and excess of furosemide, are required to shift the equilibrium in favour of deprotonated furosemide.

Crystal structures

The crystal structures of three new compounds were determined: [Zn(NH$_3$)$_2$(fur)$_2$] (**1**), NH$_4$fur (**2**) and [Zn$_3$(quin)$_4$(fur)$_2$]$_n$·2nCH$_3$OH (**3**). In the mononuclear complex [Zn(NH$_3$)$_2$(fur)$_2$] (**1**), the zinc(II) ion is surrounded by two ammonia molecules and two deprotonated furosemide ligands bound in a monodentate manner *via* carboxylate oxygens. The ORTEP drawing of **1** is shown in Fig. 1. The asymmetric unit contains one half of the complex molecule, with zinc(II) positioned on a two-fold rotation axis (C_2), which generates the other half of the molecule. To evaluate the coordination geometry, the geometric parameter for four-coordinate compounds, τ_4 ($\tau_4 = (360° − (\alpha + \beta))/141°$, and α and β are the two largest angles in the four-coordinate species), was calculated for the N$_2$O$_2$ donor set to be 0.87, indicating that the geometry is almost tetrahedral.[31] The bond
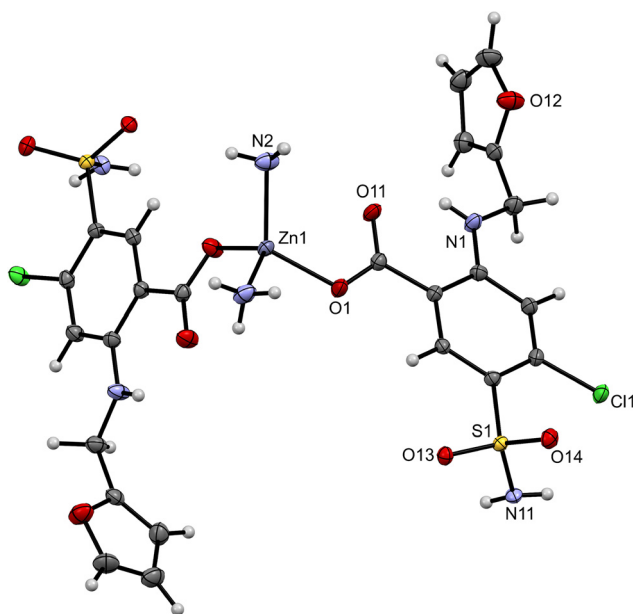
Fig. 1 Molecular structure of [Zn(NH₃)₂(fur)₂] (**1**). The displacement ellipsoids are shown at the 50% probability level. Hydrogen atoms are shown as spheres of arbitrary radii.

length between the zinc(II) ion and ammonia nitrogen is 2.013(2) Å and is comparable to values observed in similar complexes. For example, in another tetrahedral zinc(II) complex featuring two ammonia molecules and two monodentate propynoate ligands, the Zn–N bond length is 1.996(3) Å.[32] In the five-coordinated complex [Zn(quin)₂(NH₃)], the Zn–N bond is somewhat longer at 2.0281(19) Å.[16] This is to be expected, as higher coordination numbers usually result in longer bonds. The Zn–O bond to the monodentate carboxylate group of the furosemide anion measures 1.9647(17) Å, which matches with the bond lengths observed in anhydrous zinc(II) acetate, which range from 1.949(2) Å to 1.965(2) Å.[33]

Each [Zn(NH₃)₂(fur)₂] complex is hydrogen bonded to six neighbouring molecules. The list of relevant hydrogen bonds is shown in Table 2. The sulphonamide NH₂ group acts as a hydrogen bond donor, interacting with sulphonamide oxygens from two adjacent molecules. Specifically, one NH₂ hydrogen atom forms a bifurcated hydrogen bond, whereas the other is engaged in an interaction that exceeds 3.1 Å. Additionally, the hydrogen atom from ammonia forms a hydrogen bond with the carboxylate group of the adjacent furosemide ligand. The furosemide anion itself adopts a conformation which allows for an intramolecular NH···COO⁻ hydrogen bond. As a result of the hydrogen bonding motif, the complex molecules are connected into two-dimensional layers, as illustrated in Fig. 2. No significant π···π stacking interactions were observed.

Table 2 Hydrogen bond parameters for **1–3**

Compound	Hydrogen bond	D···A distance [Å]	H···A distance [Å]	D–H···A angle [°]
[Zn(NH₃)₂(fur)₂] (**1**)	NH₃···COO⁻	N···O [x, 1 + y, z] = 3.013(3)	2.16(2)	175(4)
	NH₂···SO₂	N···O [x, −1 + y, z] = 2.910(3)	2.41(3)	123(3)
	NH₂···SO₂	N···O [0.5 − x, −0.5 + y, 0.5 − z] = 2.931(3)	2.20(3)	155(3)
	NH···COO⁻ ᵃ	N···O = 2.663(3)	2.05(3)	134(3)
NH₄fur (**2**)	NH₄⁺···COO⁻	N···O = 2.779(2)	1.90(3)	173(3)
	NH₄⁺···COO⁻	N···O [1 − x, −0.5 + y, 1.5 − z] = 2.902(3)	2.06(4)	163(3)
	NH₄⁺···COO⁻	N···O [x, −1 + y, z] = 2.899(3)	1.97(3)	169(3)
	NH₄⁺···SO₂	N···O [2 − x, −1.5 + y, 1.5 − z] = 2.839(3)	2.18(3)	128(3)
	NH₄⁺···SO₂	N···O [2 − x, −0.5 + y, 1.5 − z] = 3.029(3)	2.41(3)	125(3)
	NH₂···SO₂	N···O [x, −1 + y, z] = 3.025(3)	2.41(4)	134(3)
	NH₂···COO⁻	N···O [1 + x, 1 + y, z] = 2.858(3)	1.98(3)	163(3)
	NH···COO⁻ ᵃ	N···O = 2.670(3)	1.99(3)	134(3)
[Zn₃(quin)₄(fur)₂]ₙ·2nCH₃OH (**3**)	NH₂(fur⁻)···OH(CH₃OH)	N···O [x, 1 + y, z] = 2.795(3)	1.97(4)	176(3)
	OH(CH₃OH)···COO⁻(fur⁻)	O···O = 2.721(2)	1.85(4)	168(4)
	NH(fur⁻)···COO⁻(fur⁻)ᵃ	N···O = 2.682(2)	1.99(3)	137(2)

ᵃ Intramolecular hydrogen bonds.

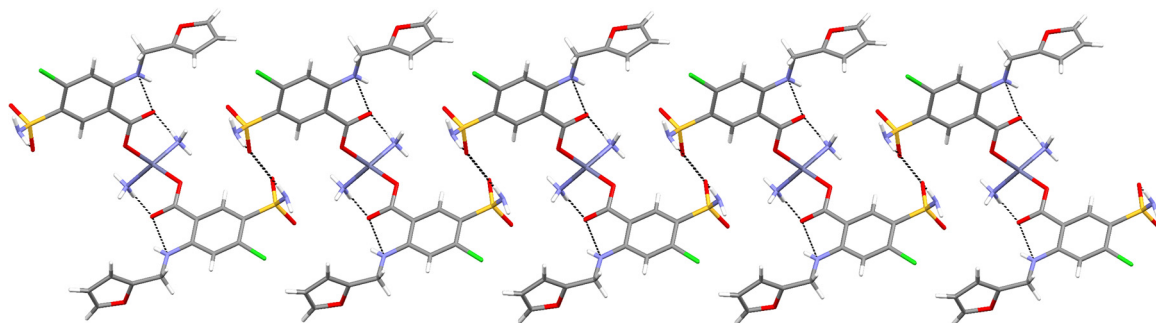
Fig. 2 Hydrogen bonding pattern in [Zn(NH₃)₂(fur)₂] (**1**). Complex molecules are linked into supramolecular layers. A view along the layer.
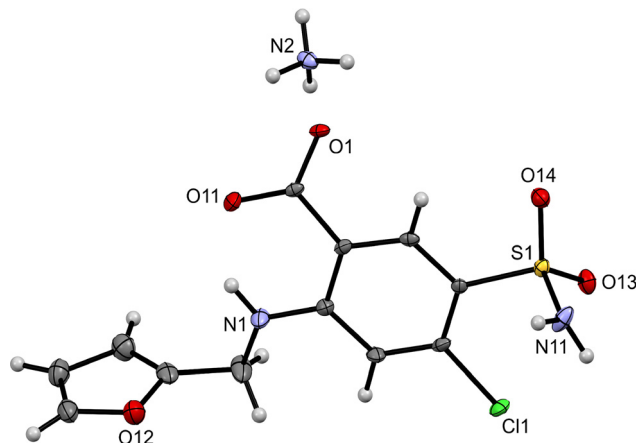
Fig. 3 ORTEP diagram of NH$_4$fur (**2**). The displacement ellipsoids are shown at the 50% probability level. Hydrogen atoms are shown as spheres of arbitrary radii.

The layers stack one upon another along the *c*-crystallographic axis (ESI,† Fig. S3).

The crystal structure of the ionic compound NH$_4$fur (**2**) consists of ammonium cations and furosemide anions (Fig. 3) that are hydrogen bonded to supramolecular layers (ESI,† Fig. S4). These layers are coplanar with the *ab* plane and stack along the *c*-axis. A notable structural feature is the significant deviation of the carboxylate group from planarity, as indicated by the dihedral angle between the carboxylate and phenyl rings, measured as 20.3(3)°. Once again, an intramolecular NH···COO⁻ hydrogen bond is observed within the furosemide anion, further stabilizing the structure.

The most intriguing compound is [Zn$_3$(quin)$_4$(fur)$_2$]$_n$·2nCH$_3$OH (**3**), a methanol solvate of a one-dimensional coordination polymer. The asymmetric unit of **3** consists of two quinaldinates, one deprotonated furosemide and two zinc(II) ions. One of the zinc(II) ions is positioned on a two-fold rotation axis and has an occupancy of 0.5. The two zinc(II) ions exhibit different

coordination environments, as illustrated in the ORTEP drawings in Fig. 4. The first zinc(II) centre is five-coordinated with two *N,O*-bidentate chelating quinaldinates and one furosemide anion that is bound in a monodentate manner *via* its carboxylate oxygen. The bond between zinc(II) and the other carboxylate oxygen is too long (2.9227(15) Å) to be considered a coordination bond. The N$_2$O$_3$ donor set has a τ_5 value of 0.37. The geometry is closer to the square pyramidal than to trigonal bipyramidal.[34] The second zinc(II) ion is four-coordinated with four quinaldinates bound in a monodentate fashion through carboxylate oxygens. A τ_4 value of 0.83 suggests a slightly distorted tetrahedral geometry.[31] Overall, the furosemide anion acts as a terminal ligand, while quinaldinate functions as a bridging ligand, linking the zinc(II) ions into infinite polymeric chains (Fig. 5). The quinaldinate ligand engages all three donor atoms in coordination with two metal centres, as depicted in Scheme 3. This coordination mode is relatively rare, with only a few examples reported in the CSD.[9] One of the rare examples is a one-dimensional copper(II) coordination polymer, [Cu(quin)$_2$]$_n$.[35] The lengths of coordination bonds in **3** are summarized in Table 3. The bond length of the zinc(II)-to-furosemide anion falls within the range observed for anhydrous zinc(II) acetate.[33] The Zn–O bond length for monodentate carboxylate coordination of the furosemide anion in the known six-coordinated zinc(II) complex was 1.9912(19).[15] The Zn–N and Zn–O bonds for the bidentate chelating quinaldinate are comparable to those of known compounds,[17] whereas the monodentate carboxylate coordination of quinaldinate leads to slightly shorter bonds (1.9441(12) Å and 1.9518(12) Å). The monodentate carboxylate binding mode is observed in a four-coordinated zinc(II) environment; therefore, shorter bonds are expected.[17]

Polymeric chains in **3** run along the *b*-axis. Methanol molecules are hydrogen bonded to the furosemide anions in these chains (Table 2 and Fig. 5). Once again, an intramolecular hydrogen bond is observed within the furosemide anion. The quinaldinate ligand does not participate in hydrogen bonds because all three hydrogen bond acceptors participate in coordination with metal ions. Quinaldinate participates in intermolecular interactions only *via* π···π
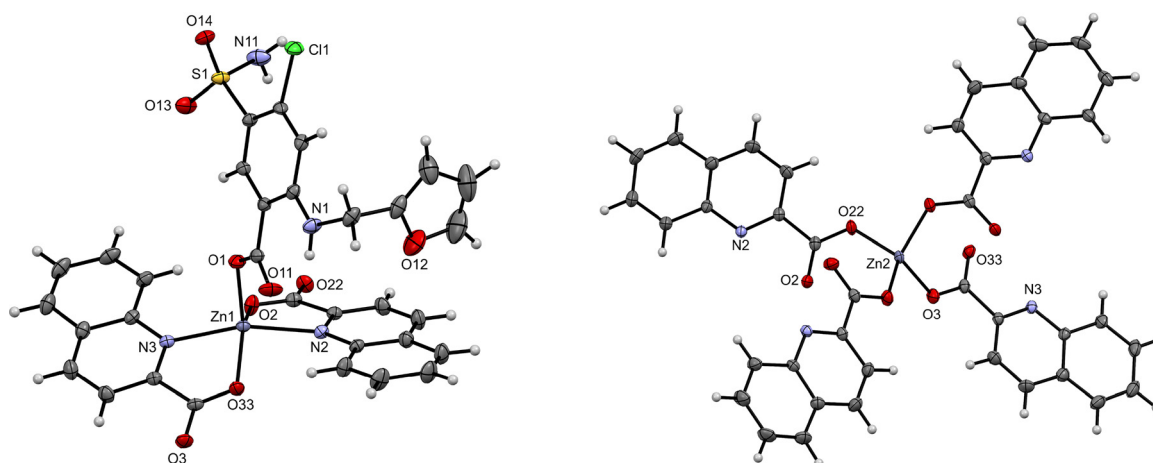

Fig. 4 Drawings of coordination environments of five-coordinated (left) and four-coordinated (right) zinc(II) ions in [Zn$_3$(quin)$_4$(fur)$_2$]$_n$·2nCH$_3$OH (**3**). The displacement ellipsoids are shown at the 50% probability level. Hydrogen atoms are shown as spheres of arbitrary radii.

This journal is © The Royal Society of Chemistry and the Centre National de la Recherche Scientifique 2025
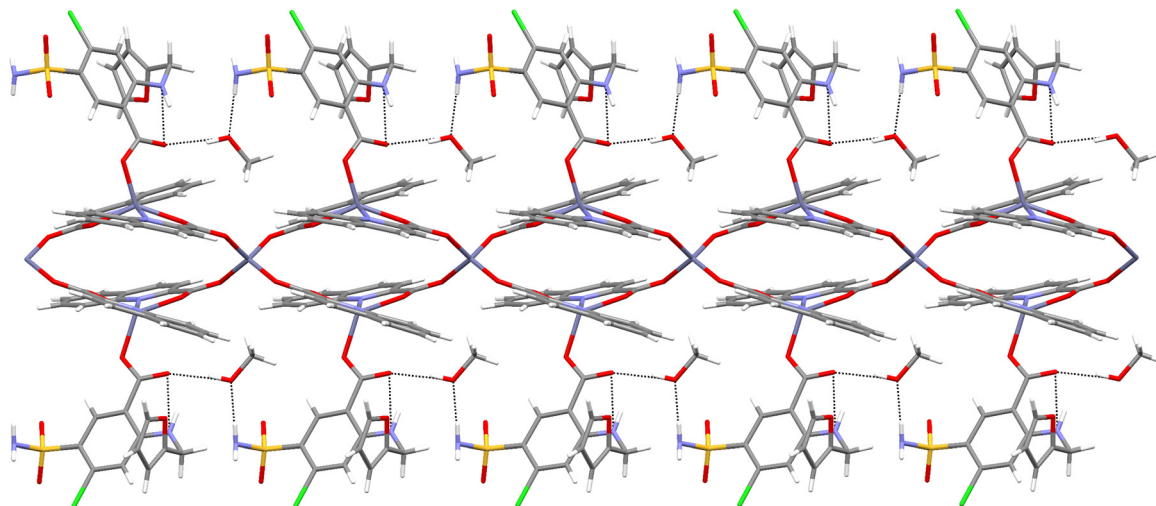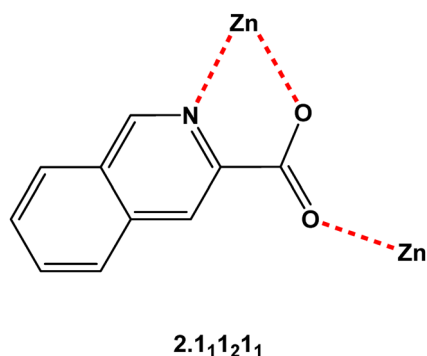
Fig. 5 1D-coordination polymer $[Zn_3(quin)_4(fur)_2]_n$ with hydrogen bonded methanol molecules.

stacking. Within the chain, $\pi \cdots \pi$ stacking interactions occur between quinaldinate ligands (arene$\cdots$pyridine type, centroid$\cdots$centroid distance = 3.841 Å, interplanar angle = 8.447°, shift distance = 1.267 Å and pyridine$\cdots$pyridine type, centroid$\cdots$centroid distance = 3.741 Å, interplanar angle = 5.412°, shift distance = 0.610 Å). The chains pack in a parallel fashion, with each chain closely surrounded by four others (Fig. 6). Polymeric chains are held together with $\pi \cdots \pi$ stacking interactions between quinaldinate ligands (arene$\cdots$pyridine type, centroid$\cdots$centroid distance = 3.763 Å, interplanar angle = 3.251°, shift distance = 1.439 Å and pyridine$\cdots$pyridine type, centroid$\cdots$centroid distance = 3.824 Å, interplanar angle = 0.000°, shift distance = 1.572 Å).[37]

2.1₁1₂1₁

Scheme 3 Quinaldinate binding mode with the corresponding Harris notation.[36]

Table 3 Relevant bond lengths [Å] in **3**

Bond	Length [Å]
Zn–O (fur⁻)	1.9631(12)
Zn–N (quin⁻)	2.1855(14), 2.1939(13)
Zn–O (quin⁻, bidentate to Zn1)	2.0212(12), 2.0258(12)
Zn–O (quin⁻, monodentate to Zn2)	1.9441(12), 1.9518(12)

IR spectroscopy

The infrared spectra of $[Zn(NH_3)_2(fur)_2]$ (**1**), NH_4fur (**2**) and $[Zn_3(quin)_4(fur)_2]_n \cdot 2nCH_3OH$ (**3**) form part of the ESI.† With all spectra being rather complex, the following discussion is limited only to the most prominent absorption bands of a particular structural element. The literature reports an exhaustive study of the infrared and Raman spectra of free furosemide, corroborated with theoretical DFT calculations.[38] Compounds **1**–**3** contain fur⁻, a furosemide form with a deprotonated COOH group, which acts either as a ligand (compounds **1** and **3**) or as a counter-anion (compound **2**). Their infrared spectra reflect the absence of the COOH proton. In free furosemide, the C=O stretching vibration absorbs at 1668 cm⁻¹. Conversely, the spectra of **1**–**3** display a very intense band at a lower frequency, i.e., 1612 cm⁻¹ (**1**), 1606 cm⁻¹ (**2**) and 1605 cm⁻¹ (**3**). Frequencies of the $\nu_{as}(COO^-)$ and $\nu_s(COO^-)$ vibrations are known to be sensitive to the carboxylate binding mode.[39] In the spectrum of **2**, an ammonium salt of fur⁻, the characteristic carboxylate bands occur at 1606 and 1447 cm⁻¹. The $\nu_{as}(COO^-)$–$\nu_s(COO^-)$ difference amounts to 159 cm⁻¹ which is a typical value for carboxylate salts.[40] In compound **1** with the furosemide carboxylate moiety engaged in a monodentate coordination, the carboxylate absorption bands are wide apart, i.e., at 1612 and 1378 cm⁻¹. The resulting difference, known also as a splitting value,[39] is 234 cm⁻¹. Compound **3** contains two types of carboxylate ligands, apart from the monodentate carboxylate of the fur⁻ ligand, also the carboxylate of quinaldinate whose binding mode is depicted in Scheme 3. Consequently, the spectrum of **3** is more complex. The 1605 cm⁻¹ band in **3** may be ascribed to the $\nu_{as}(COO^-)$ vibration, whereas three bands appear in the $\nu_s(COO^-)$ spectral region, at 1469, 1415 and 1379 cm⁻¹.

The most intense band in the spectrum of free furosemide, i.e., at 1140 cm⁻¹, is attributed to the symmetric stretching of the S=O bonds in the sulphonamide group. The $\nu_{as}(SO_2)$ vibration absorbs at 1318 cm⁻¹.[38] The vibrations of the S=O bonds leave a characteristic

imprint also over the spectra of **1–3**. The $\nu_s(SO_2)$ vibration is seen as a strong band at 1153 cm^{-1} (compound **1**), 1159 cm^{-1} (**2**) or 1165 cm^{-1} (**3**). In **1**, the asymmetric stretching vibration may be associated with the 1311 cm^{-1} band. A very intense peak at 1302 cm^{-1} is observed in the spectrum of **2**. For compound **3**, two bands are displayed in this region, at 1341 cm^{-1} and at 1298 cm^{-1}.

The NH$_2$ and NH groups in furosemide ions are seen by the absorptions in two spectral regions. In the region of N–H stretching vibrations, two sharp bands of medium intensity are revealed in the spectra of **1** and **2**. For example, the spectrum of **1** has peaks at 3371 and 3254 cm^{-1}. The spectrum of **3** is characterized by only one, broad and weak band at 3276 cm^{-1}. The N–H deformation vibration occurs as a very intense absorption band at 1555 cm^{-1} in the spectra of all three.

The assignation of the vibrational spectra of free furosemide further states that a strong absorption band at 578 cm^{-1} finds its origin in the out-of-plane O–H vibration.[38] A rather intense band at *ca.* 580 cm^{-1}, observed in the infrared spectra of **1–3**, disputes the latter. With compounds **1–3** containing COO$^-$ and not COOH groups, the origin of this band must lie elsewhere. It is to be noted that this absorption band falls within a reported spectral range for the ν(C–Cl) vibrations (785–540 cm^{-1}).[41] In view of a few more peaks of similar intensity in the vicinity, the assignation is not unambiguous.

With [Zn(NH$_3$)$_2$(fur)$_2$] (**1**) containing coordinated ammonia, its spectrum was compared to the spectrum of another complex with ammonia. The spectrum of [Zn(quin)$_2$(NH$_3$)] has characteristic ammonia bands at 3282, 3212, 3159 and 1260 cm^{-1}.[16] Based on this comparison, a higher intensity of the 3254 cm^{-1} band in **1** could be due to the ν(N–H) vibrations of coordinated ammonia. Furthermore, the strong 1254 cm^{-1} peak in **1** could be ascribed to bending vibrations of ammonia.

NH$_4$fur (**2**) is an ammonium salt. The most characteristic feature of ammonium ions are two broad bands centred at *ca.* 2960 and 2835 cm^{-1} which could be assigned as N–H stretching vibrations of the hydrogen bonded ammonium ions.

Sharp bands at 3407 and 1029 cm^{-1} in the spectrum of [Zn$_3$(quin)$_4$(fur)$_2$]$_n$·2nCH$_3$OH (**3**) confirm the presence of methanol solvent molecules. As the solid slowly loses the solvent molecules, the intensity of these bands diminishes with time. The high-frequency band is associated with the ν(O–H) vibration, and the low-frequency one with the ν(C–O) vibration of primary alcohol.

^{1}H NMR spectroscopy

^{1}H NMR spectra of DMSO-d_6 solutions of **1** and **3** are consistent with the compositions of both compounds. In order to assist with the assignations, the spectrum of [Zn(NH$_3$)$_2$(fur)$_2$] (**1**) was compared to that of free furosemide and literature assignations were also consulted.[42] The comparison has a noteworthy shortcoming: whereas **1** contains a form of furosemide with a deprotonated COOH group, the carboxyl group in free furosemide still bears a proton. The ^{1}H NMR spectrum of free furosemide reveals nine resonances. The signal for the COOH proton appears at 13.36 ppm and the signal for the NH$_2$ protons at 7.34 ppm. The spectrum of **1** reveals seven resonances. Apart from the signal for the COOH proton, it also lacks the one for the exchangeable NH$_2$ protons. The addition of a small amount of furosemide to the solution of **1** results in minor shifts of all resonances and in the appearance of a new signal at 7.17 ppm. The latter can be ascribed to the NH$_2$ protons. The comparison of the spectra of **1** and free furosemide reveals a downfield shift in the NH proton resonance. In the spectrum of **1**, it appears at 9.46 ppm, whereas for free furosemide it appears at 8.63 ppm. The ^{1}H NMR spectra of ammine complexes sometimes reveal signals of the exchangeable NH$_3$ protons, as exemplified by the 3.49 ppm resonance for [Zn(quin)$_2$(NH$_3$)].[16] No such signal could be found in the spectrum of **1**.

With the exceptions of methanol resonances, most of the resonances in the spectrum of [Zn$_3$(quin)$_4$(fur)$_2$]$_n$·2nCH$_3$OH (**3**) are broad. Nevertheless, their integrals match nicely with the
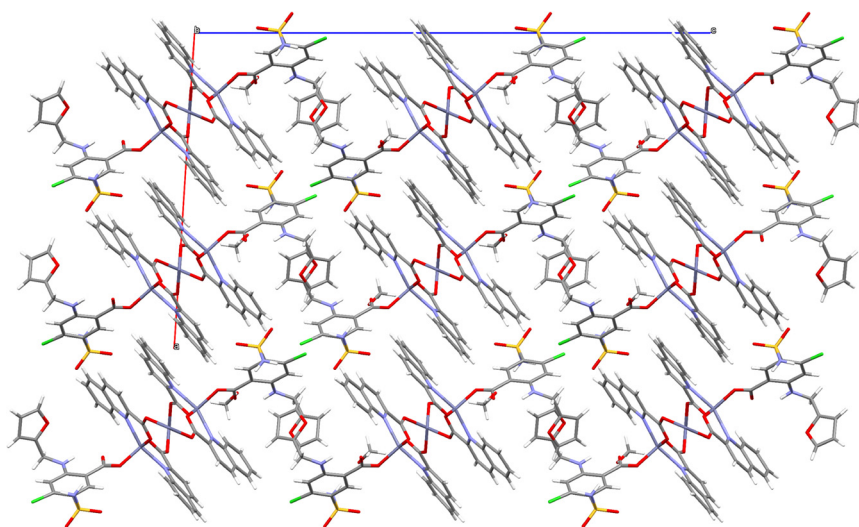
Fig. 6 Packing of polymeric chains in [Zn$_3$(quin)$_4$(fur)$_2$]$_n$·2nCH$_3$OH (**3**): a view along chains.

Table 4 Results of antibacterial testing

Compound	MIC [μg mL^{-1}]					
	E. coli	*S. aureus*	*P. aeruginosa*	*Proteus mirabilis*	*Bacillus subtilis*	*S. epidermidis*
Zinc(II) acetate dihydrate	>128	>128	>128	>128	>128	32
Furosemide	>128	>128	>128	>128	>128	>128
Quinaldic acid	>128	>128	>128	>128	>128	>128
[Zn(NH$_3$)$_2$(fur)$_2$] (**1**)	>128	>128	>128	>128	>128	128
[Zn$_3$(quin)$_4$(fur)$_2$]$_n$·2nCH$_3$OH (**3**)	>128	>128	>128	>128	>128	64

composition of **3**. Methanol signals appear at 4.10 and 3.17 ppm. Quinaldinates may be seen as ten signals in the 8.82–7.72 ppm interval. Very similar chemical shifts were observed for other zinc(II) complexes with quinaldinate.[20] For these, either five or six signals are typically shown. The number of signals for **3** suggests two quinaldinates in slightly different environments. Furosemide ligands display eight resonances. Interestingly, there is a NH$_2$ protons' resonance at 7.19 ppm. The NH proton which resonates at 9.10 ppm experiences a smaller downfield shift than the one in **1**.

Antibacterial activity

Antibacterial activities of compounds were tested according to the European Committee for Antibacterial Susceptibility Testing recommendations[43] and the Clinical Laboratory Standards Institute protocol. The results are summarized in Table 4 in the form of minimum inhibitory concentrations (MICs) in μg mL^{-1} for the tested bacterial strains. In general, compounds did not show any promising antibacterial activity against the panel of bacteria. However, zinc(II) acetate dihydrate and the coordination polymer [Zn$_3$(quin)$_4$(fur)$_2$]$_n$·2nCH$_3$OH (**3**) showed the modest antibacterial activity against *S. epidermidis*. *Staphylococcus epidermidis* is a Gram-positive bacterium and a key component of the human skin microbiota. While typically commensal, it is a major cause of nosocomial infections, especially in immunocompromised patients and those with implanted medical devices.[44,45] Its ability to form biofilms on surfaces like catheters and prosthetics enhances its antibiotic resistance and immune evasion, complicating treatment.[46] Methicillin-resistant *S. epidermidis* is increasingly prevalent in hospitals, highlighting the need for strategies to manage its dual role as both a beneficial microbe and an opportunistic pathogen.[47] Previously prepared [Zn(fur)$_2$(H$_2$O)(2,2'-bipy)] has also been tested for its activity against the same series of bacteria.[15] The bipyridine complex showed activity against *Proteus mirabilis* and *S. aureus* which was not stronger than for bipyridine itself in either case.

Conclusions

The investigation of zinc(II) coordination chemistry with the furosemide anion led to the preparation of two novel zinc(II) complexes. In aqueous ammonia, zinc(II) oxide or chloride reacted with furosemide to form a mononuclear, tetrahedrally coordinated [Zn(NH$_3$)$_2$(fur)$_2$] (**1**). The furosemide anion coordinated with zinc(II) in a monodentate manner *via* carboxylate oxygen. When furosemide was reacted with [Zn(quin)$_2$(H$_2$O)]

under harsher reaction conditions (105 °C in an autoclave), the one-dimensional coordination polymer [Zn$_3$(quin)$_4$(fur)$_2$]$_n$·2nCH$_3$OH (**3**) was formed. The coordination mode of the furosemide anion was the same as in **1**. Quinaldinate fully utilized its binding potential by binding to two zinc(II) ions *via* all three donors. Testing of **3** against *S. epidermidis* showed moderate antibacterial activity.

Data availability

The data supporting this article have been included as part of the ESI.† Crystallographic data for **1**, **2** and **3** have been deposited at the CCDC under the deposition numbers 2420534–2420536† and can be obtained from https://www.ccdc.cam.ac.uk/structures/.

Conflicts of interest

There are no conflicts to declare.

References

1 G. E. Granero, M. R. Longhi, M. J. Mora, H. E. Junginger, K. K. Midha, V. P. Shah, S. Stavchansky, J. B. Dressman and D. M. Barends, *J. Pharm. Sci.*, 2010, **99**, 2544–2556.

2 X. Huang, E. Dorhout Mees, P. Vos, S. Hamza and B. Braam, *Am. J. Physiol. Renal. Physiol.*, 2016, **310**, F958–F971.

3 N. J. Babu, S. Cherukuvada, R. Thakuria and A. Nangia, *Cryst. Growth Des.*, 2010, **10**, 1979–1989.

4 M. Lindenberg, S. Kopp and J. B. Dressman, *Eur. J. Pharm. Biopharm.*, 2004, **58**, 265–278.

5 U. B. Rao Khandavilli, S. Gangavaram, N. Rajesh Goud, S. Cherukuvada, S. Raghavender, A. Nangia, S. G. Manjunatha, S. Nambiar and S. Pal, *CrystEngComm*, 2014, **16**, 4842–4852.

6 J. Abraham Miranda, C. Garnero, A. K. Chattah, Y. Santiago de Oliveira, A. P. Ayala and M. R. Longhi, *Cryst. Growth Des.*, 2019, **19**, 2060–2068.

7 Ö. Almarsson and M. J. Zaworotko, *Chem. Commun.*, 2004, 1889–1896.

8 N. R. Goud, S. Gangavaram, K. Suresh, S. Pal, S. G. Manjunatha, S. Nambiar and A. Nangia, *J. Pharm. Sci.*, 2012, **101**, 664–680.

9 C. R. Groom, I. J. Bruno, M. P. Lightfoot and S. C. Ward, *Acta Crystallogr., Sect. B*, 2016, **72**, 171–179.

10 S. Karami, Y. Li, D. S. Hughes, M. B. Hursthouse, A. E. Russell, T. L. Threlfall, M. Claybourn and R. Roberts, *Acta Crystallogr., Sect. B*, 2006, **62**, 689–691.

11 A. J. Cruz-Cabeza and J. Bernstein, *Chem. Rev.*, 2014, **114**, 2170–2191.

12 J. Lamotte, H. Campsteyn, L. Dupont and M. Vermeire, *Acta Crystallogr., Sect. B*, 1978, **34**, 1657–1661.

13 Y. Matsuda and E. Tatsumi, *Int. J. Pharm.*, 1990, **60**, 11–26.

14 P. Bontchev, H. Kadum, G. Gochev, B. Evtimova, J. Macicek and C. Nachev, *Polyhedron*, 1992, **11**, 1973–1980.

15 G. Raymoni and H. Abu Ali, *Appl. Organomet. Chem.*, 2019, **33**, e4680.

16 N. Podjed, P. Stare, R. Cerc Korošec, M. M. Alcaide, J. López-Serrano and B. Modec, *New J. Chem.*, 2020, **44**, 387–400.

17 N. Podjed, B. Modec, M. M. Alcaide and J. López-Serrano, *RSC Adv.*, 2020, **10**, 18200–18221.

18 N. Podjed and B. Modec, *New J. Chem.*, 2022, **46**, 23225–23238.

19 N. Podjed and B. Modec, *J. Mol. Struct.*, 2023, **1284**, 135457.

20 N. Podjed, J. Košmrlj and B. Modec, *New J. Chem.*, 2024, **48**, 8844–8859.

21 D. B. G. Williams and M. Lawton, *J. Org. Chem.*, 2010, **75**, 8351–8354.

22 H. E. Gottlieb, V. Kotlyar and A. Nudelman, *J. Org. Chem.*, 1997, **62**, 7512–7515.

23 M. R. Willcott, *J. Am. Chem. Soc.*, 2009, **131**, 13180.

24 Agilent, *CrysAlis PRO*, Agilent Technologies Ltd, Yarnton, Oxfordshire, England, 2014.

25 G. M. Sheldrick, *Acta Crystallogr., Sect. A*, 2015, **71**, 3–8.

26 O. V. Dolomanov, L. J. Bourhis, R. J. Gildea, J. A. K. Howard and H. Puschmann, *J. Appl. Crystallogr.*, 2009, **42**, 339–341.

27 G. M. Sheldrick, *Acta Crystallogr., Sect. C*, 2015, **71**, 3–8.

28 A. L. Spek, *Acta Crystallogr., Sect. D*, 2009, **65**, 148–155.

29 C. F. Macrae, I. Sovago, S. J. Cottrell, P. T. A. Galek, P. McCabe, E. Pidcock, M. Platings, G. P. Shields, J. S. Stevens, M. Towler and P. A. Wood, *J. Appl. Crystallogr.*, 2020, **53**, 226–235.

30 N. Okabe and Y. Muranishi, *Acta Crystallogr., Sect. E*, 2003, **59**, m244–m246.

31 L. Yang, D. R. Powell and R. P. Houser, *Dalton Trans.*, 2007, 955–964.

32 M. B. Ruth and B. M. Foxman, *Mol. Cryst. Liq. Cryst. Sci. Technol., Sect. A*, 2001, **356**, 61–69.

33 W. Clegg, I. R. Little and B. P. Straughan, *Acta Crystallogr., Sect. C*, 1986, **42**, 1701–1703.

34 A. W. Addison, T. N. Rao, J. Reedijk, J. van Rijn and G. C. Verschoor, *J. Chem. Soc., Dalton Trans.*, 1984, 1349–1356.

35 N. Podjed, B. Modec, R. Clérac, M. Rouzières, M. M. Alcaide and J. López-Serrano, *New J. Chem.*, 2022, **46**, 6899–6920.

36 R. A. Coxall, S. G. Harris, D. K. Henderson, S. Parsons, P. A. Tasker and R. E. P. Winpenny, *J. Chem. Soc., Dalton Trans.*, 2000, 2349–2356.

37 C. Janiak, *J. Chem. Soc., Dalton Trans.*, 2000, 3885–3896.

38 O. Bolukbasi and A. Yilmaz, *Vib. Spectrosc.*, 2012, **62**, 42–49.

39 G. B. Deacon and R. J. Phillips, *Coord. Chem. Rev.*, 1980, **33**, 227–250.

40 K. Nakamoto, *Infrared and Raman Spectra of Inorganic and Coordination Compounds. Part B: Applications in Coordination, Organometallic, and Bioinorganic Chemistry*, Wiley, Hoboken, NJ, 6th edn, 2009.

41 D. L. Pavia, G. M. Lampman and G. S. Kriz, *Introduction to Spectroscopy*, Thomson Learning, London, UK, 2001.

42 SDBSWeb (National Institute of Advanced Industrial Science and Technology), **https://sdbs.db.aist.go.jp**, accessed 25. 3. 2025.

43 EUCAST, Antimicrobial susceptibility testing, **https://www.eucast.org/ast_of_bacteria**, accessed 3. 2. 2025.

44 M. Otto, *Nat. Rev. Microbiol.*, 2009, **7**, 555–567.

45 M. Widerström, *J. Clin. Microbiol.*, 2016, **54**, 1679–1681.

46 S. M. Skovdal, N. P. Jørgensen and R. L. Meyer, *J. Med. Microbiol.*, 2022, **71**, 001597.

47 V. Siciliano, R. A. Passerotto, M. Chiuchiarelli, G. M. Leanza and V. Ojetti, *Life*, 2023, **13**, 1126.